FLAME EMISSION SPECTROSCOPY MEASUREMENT OF A STEAM BLAST AND AIR BLAST BURNER

by

Viktor JOZSA [*] ***and Krisztian SZTANKO***

Department of Energy Engineering, Budapest University of Technology and Economics, Budapest, Hungary

Original scientific paper
https://doi.org/10.2298/TSCI150616062J

Control and online monitoring of combustion have become critical to meet the increasingly strict pollutant emission standards. For such a purpose, optical sensing methods, like flame emission spectrometry, seem to be the most feasible technique. Spectrometry is capable to provide information about the local equivalence ratio inside the flame through the chemiluminescence intensity ratio measurement of various radicals. In the present study, a 15 kW atmospheric burner was analyzed utilizing standard diesel fuel. Its plain jet type atomizer was operated with both air and steam atomizing mediums. Up to now, injection of steam into the reaction zone has attracted less scientific attention contrary to its practical importance. Spatial plots of OH, CH*, and C_2* excited radicals were analyzed at 0.35, 0.7, and 1 bar atomization gauge pressures, utilizing both atomizing mediums. The C_2* was found to decrease strongly with increasing steam addition. The OH*/CH* and OH*/C_2* chemiluminescence intensity ratios along the axis showed a divergent behavior in all the analyzed cases. Nevertheless, CH*/C_2* chemiluminescence intensity ratio decreased only slightly, showing low sensitivity to the position of the spectrometer. The findings may be directly applied in steady operating combustion systems, i. e., gas turbines, boilers, and furnaces.*

Key words: *flame emission spectroscopy, lean combustion, premixed flame, chemiluminescence, air blast atomization, steam blast atomization*

Introduction

The continuously stricter pollutant emission regulations have forced researchers for decades to develop advanced combustion systems [1-6]. The literature identifies two primary means to achieve lower emissions. The first one is a well designed flow pattern to determine the local equivalence ratio in the flame, which is commonly referred to as dry low emission (DLE) combustion system [7]. The currently analyzed burner is a lean premixed prevaporized (LPP) one, which belongs to the DLE family. The second method is adding external fluid to the reaction zone (*e. g.*, steam, water, N_2, CO_2), which is called wet emission control. In the present paper, the two mentioned methods are combined by applying steam as an atomizing medium in an atmospheric LPP burner, which is originally designed for air blast operation.

Plenty of studies investigated water or steam injection techniques [4, 8-12], but this method is uncommon in the state-of-the-art combustion systems. Typically, water-fuel

* Corresponding author, e-mail: jozsa@energia.bme.hu

emulsion improves the atomization characteristics since the lower boiling point of the water leads to micro-explosions and results in a finer fuel spray [8, 13]. This method is utilized in several land-based power generating gas turbines in order to keep the emission of NO_x below the threshold. In industrial boilers where the steam generator is already present, steam injection to the combustion zone is more prevalent [10, 11]. Furuhata *et al.* [4] concluded that the most efficient burner configuration for steam addition from the NO_x emission point of view is neighborhood of the atomizer.

It is known for wet emission control that the effective thermal NO_x reduction requires a water-to-fuel ratio on the order of one, which is usually limited by an unacceptable increase in CO emission. Hence, the typically applied water-to-fuel ratio is 0.8-1.2 [12]. Consequently, the steam-to-fuel ratio of 0.54-1 was applied for steam blast atomization in the present paper. Thus, the H_2O content of the exhaust gas would be approximately double than that of the air blast case, considering diesel oil firing. Zhao *et al.* [14] numerically analyzed a counter-flowing air-methane reactor with and without steam addition. They found less CH and N radicals and more OH radicals comparing the two cases due to the dissociation of the H_2O. De Jager *et al.* [15] found a significantly lower atomic oxygen concentration at 2000 K adiabatic flame temperature by adding steam, leading to less NO_x production.

At laboratory scales, planar laser-induced fluorescence is commonly applied for flame diagnostics. It is often combined with particle image velocimetry to investigate the flame-vortex-acoustic interactions, see, *e. g.*, [16-18]. However, the state-of-the-art development of online flame monitoring methods focuses on the application of flame emission spectroscopy (FES) due to its low cost and robustness [19-29]. The theoretical framework of FES for equivalence ratio monitoring was developed for laminar premixed flames, especially for methane-air flame [24-29]. Despite to this fact, it is also applicable to turbulent flames at industrial scales [19-21]. Interestingly, only a few papers discuss FES of liquid fuel combustion. However, most of them investigate reciprocating engines [30-32], but not steady--operating turbulent flames.

In the present paper, air-to-fuel equivalence ratio, λ, is used instead of the more common fuel-to-air equivalence ratio, ϕ. For determining λ, the chemiluminescence emission of typically OH*, CH*, CO_2*, C_2*, or an entire spectrum in the UV-VIS range is measured [24]. Mostly the CH*/OH* is used for determining the local fuel-to-air equivalence ratio since it shows a power law relation with both ϕ and operational pressure [20, 26, 27]. Furthermore, the mass flow rate of the premixed fuel was found to be proportional to the chemiluminescence intensity [20, 26, 27]. Therefore, it is less important to test a burner at different loadings at the same λ and so it is neglected in the presented measurement series.

Generally, there are a lot more papers on atmospheric combustion experiments than on measurements at elevated pressure. Their reason is that if the combustion performance is satisfactory at lower pressures, the situation will only improve at elevated pressures [7, 33]. It is in line with the experiments of Higgins *et al.* [26, 27].

The novelty of the present paper is the spectroscopic analysis of a steam blast burner, which is absent from the technical literature, according to the best knowledge of the authors. The same test series were carried out by air blast atomization for comparison reasons. Furthermore, the investigated flame is an entirely turbulent one, which is widely applied in practical combustion systems, *e. g.*, gas turbines, boilers, and furnaces. Kun-Balog and Sztanko [34] have investigated the same burner from pollutant emission point of view, also the current paper presents the corresponding FES analysis.

Details of the measurement

Measurement configuration

The core of the measurements was an LPP burner, shown in fig. 1. It is identical to those that are used in the Capstone C-30 micro gas turbine. The diameter of the mixing tube is 26.8 mm, and its length is 75.5 mm. It has four circular and fifteen rectangular holes. The latter ones have 45° inlet angle in order to swirl the combustion air. The fuel enters through the inner pipe (0.4 mm internal diameter). The plain jet atomizer is concentric with that (0.6 mm inner and 1.6 mm outer diameter).

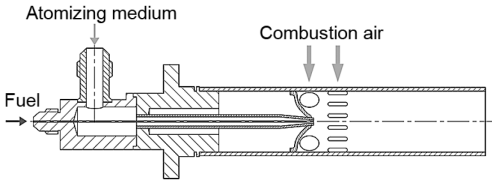

Figure 1. The Capstone C-30 micro gas turbine burner

Figure 2(a) shows the atmospheric test rig. The combustion air was delivered by a fan equipped with a frequency inverter. A rotameter (3-30 m^3/h measurement range, 2.5% accuracy class according to VDI/VDE 3513) was used for monitoring the volumetric flow rate of the combustion air. Then the combustion air was heated up to 400 °C in a relay-controlled preheater by four 1000 W heater filaments.

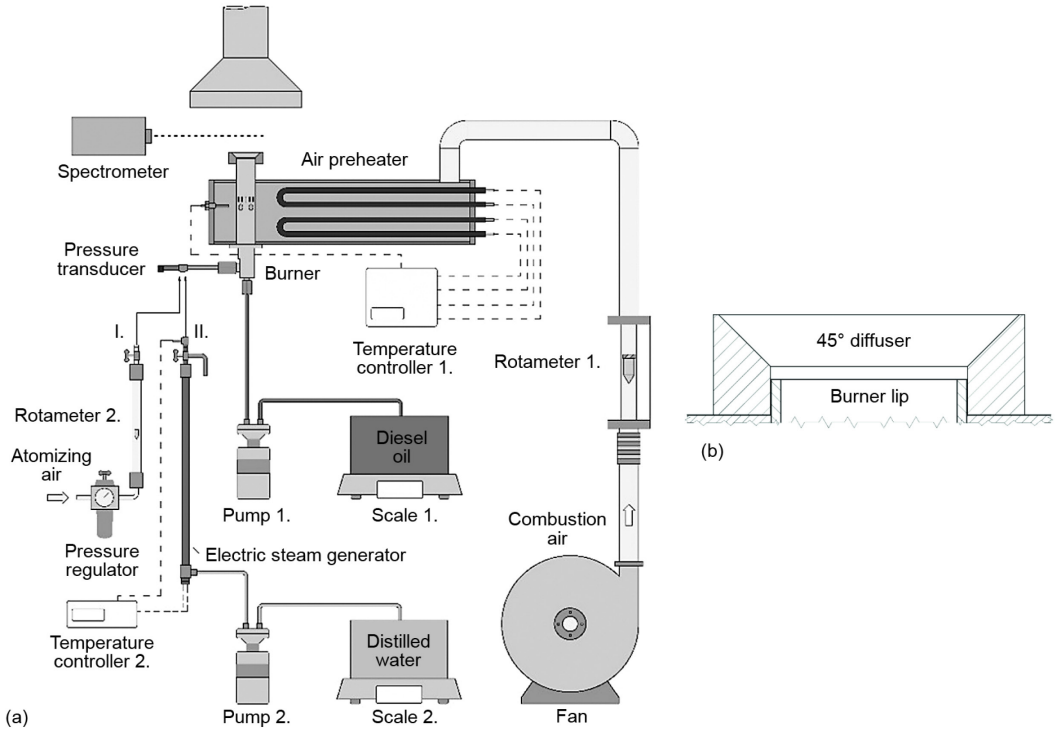

Figure 2. Burner test rig (a) and the diverging nozzle (b)

The atomizing air pressure was set by a regulator valve. A second rotameter (3-30 Lpm measurement range, 4% accuracy class according to VDI/VDE 3513) measured the volumetric flow rate of the atomizing air. A certified scale measured the mass flow rate of the

fuel (0.2 g uncertainty, approved by National Office of Measures, Hungary), averaging the consumption over 30 seconds. The hot exhaust gas was finally delivered to the stack.

For steam blast atomization, two PID-controlled 1.5 kW electric heater tubes boiled the water to produce the 200 °C temperature superheated steam. Water consumption was measured with a second scale (identical to the aforementioned one). Naturally, distilled water was used during the experiments to avoid contamination in the tiny nozzle of the atomizer. Since flame stabilization was not achieved with the original burner, a subsequent diverging nozzle was necessary to achieve stable combustion, shown in fig. 2(b). Similarly, the diverging nozzle was used during air blast atomization as well. More details about the measurement system can be found in the literature [34, 35].

Measurement conditions

In the present study, experiments were performed at three atomization gauge pressures: 0.35, 0.7, and 1.0 bar based on the findings of Kun-Balog and Sztanko [34]. The utilized fuel was standard diesel oil (according to EN 590:2014) with a constant 0.35 g/s mass flow rate for each case, which is equal to 15 kW combustion power. The target λ was 1.15 in the mixing tube that remained constant during the measurements. Hence, combustion airflow rate was 20.8 kg/h. In the case of steam blast atomization, there were higher mass flow rates present in the mixing tube in order to maintain the same λ. The mass flow rate of combustion air was reduced to maintain a constant λ in the mixing tube while the atomizing pressure was increased. The ambient temperature was 20 °C, which was required for the correction of the rotameters.

The FES measurement

A fixed spectrometer was used for the FES measurement. The focal length of the 20 mm diameter quartz objective was fixed at 0.5 m. It establishes a line-of-sight measurement with 5 mm in diameter at the focus. The spectrometer has an S3904-1024Q type n-channel metal-oxide semiconductor field-effect transistor detector. The investigated spectral range was 260-580 nm (UV-VIS, 0.3125 nm wavelength resolution). While the detector has a non-uniform voltage-wavelength characteristics, the results may differ from that of the literature as other researchers preferred charge-couple device detectors [19-29]. Typically, no further information is provided regarding their sensitivity correction. However, the measured intensities presented in the current paper were corrected based on the sensitivity characteristic of the detector given by the manufacturer. The integration time was set to 100 ms. The intensity of 64 data sets, hence 6.4 seconds, were averaged at each measurement point. Currently, chemiluminescence emission of OH*, CH*, and C_2* excited radicals are being investigated at 309, 430, and 516 nm, respectively. The wavelength calibration of the spectrometer was carried out with an Avantes AvaLight mercury-argon lamp, achieving R^2 of 0.999997. Furthermore, it is assumed that the uncertainty of the spectral intensity is unity. The combined expanded uncertainties are shown in the respective figures. Finally, the uncertainty of the positioning system of the spectrometer is 1 mm both horizontally and vertically. Further details of the spectrometer can be found in the literature [36, 37].

Results and discussion

Three recorded chemiluminescent intensity spectra are presented in fig. 3, which were recorded above the burner lip. The three most intense peaks correspond to OH*, CH*, and C_2* at 309, 430, and 516 nm, respectively. However, the rest of the paper deal with only $\lambda = 1.15$, a rich flame spectrum at $\lambda = 0.7$ is also shown in fig. 3 for comparison reasons. Only steam blast

atomization at 1 bar atomization gauge pressure and air blast atomization at 0.35 bar atomization gauge pressure are indicated while other measured spectra fell in between them at λ = 1.15. However, at λ = 0.7 the appearing soot particles superpose a nearly black body emission characteristic starting from 400 nm. It is clear that at λ = 1.15 the spectra are free from such an effect. Consequently, there is no need for further spectrum correction due to the presence of soot.

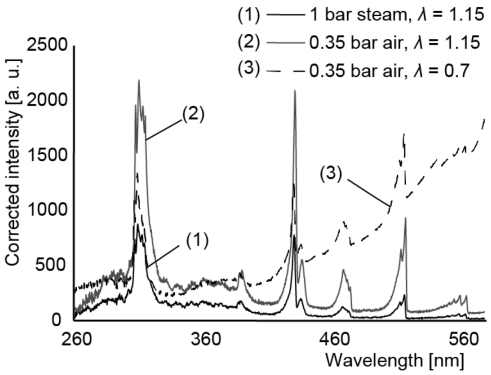

Figure 3. Effect of λ on the emission spectra through the appearance of soot

Air blast atomization resulted in Reynolds number of 8550 in the mixing tube at λ = 1.15. As for the steam blast configuration, 0.35, 0.7, and 1 bar atomization gauge pressure resulted in Re = 8992, 9206, and 9375, respectively. The application of a mixing tube and a subsequent diffusor after it ensured a flame with roots inside the tube. The calculated adiabatic flame temperature was 1941 °C for air blast atomization and 1857, 1820, and 1792 °C for the steam blast atomization cases at 0.35, 0.7, and 1 bar atomization gauge pressures, respectively, by neglecting the entrained ambient air. To retain the adiabatic flame temperature at constant in such a situation, the inlet steam temperature of 1500 °C would be required while steam has higher specific heat than air. Obviously, it was out of the capabilities of the measurement system. However, *e. g.*, by applying diluents it is possible to maintain the same adiabatic flame temperature, the current investigation focuses on the changeover of atomizing medium from air to steam at constant λ and similar swirl number.

Intensity maps

At each atomization pressure value, both steam and air blast atomization were examined horizontally at thirteen points and vertically at nineteen points, with 5 mm spacing in both directions. For post-processing, linear interpolation was used on the contour plots to show a better visual representation. Each plot was halved vertically and joined together with a halved photograph to improve the understanding and interpretation of the observed flame structure, as shown in figs. 4, 5, and 6. The intensity range was set from 0-700 in all plots, except the steam blast and air blast atomization cases at 0.35 bar atomization gauge pressure. Therefore, in fig. 4(b) the maximum value was set to 1300 units. Figures 4, 5, and 6 neglect the background noise correction arising mainly from CO_2*, but the dark current correction was performed. This intermediate analysis shows qualitative information only. However, this step is often skipped in the literature showing only the fully corrected data sets, see, *e. g.*, [22-24]. The analysis of the fully corrected intensity ratios is discussed in chapter *Investigation of intensity ratios.*

At 0.35 bar atomization gauge pressure, all the OH*, CH*, and C_2* chemiluminescence intensities were lower in the steam blast atomization cases compared to those of the air blast ones, as shown in fig. 4, probably due to the lower adiabatic flame temperature. Furthermore, the flame was bluish and fewer flares were observed. A possible explanation for this phenomenon is the enhanced heat transfer rate near the atomizer due to the condensing steam on the surface of the droplets, leading to more homogeneous combustion.

The results of the steam blast and air blast atomization at 0.7 and 1 bar atomization gauge pressures are shown in figs. 5 and 6. The OH* and CH* chemiluminescence intensities

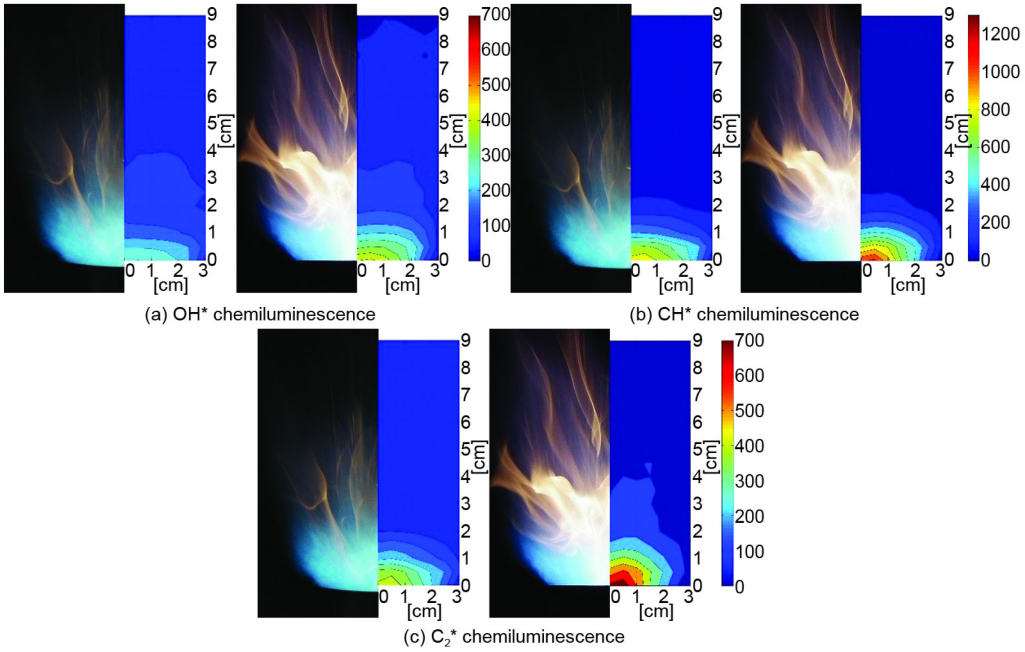

Figure 4. Raw OH*, CH*, C_2* chemiluminescence distribution with a comparison of steam blast (left) and air blast atomization (right) at a 0.35 bar atomization gauge pressure
(*for color image see journal web site*)

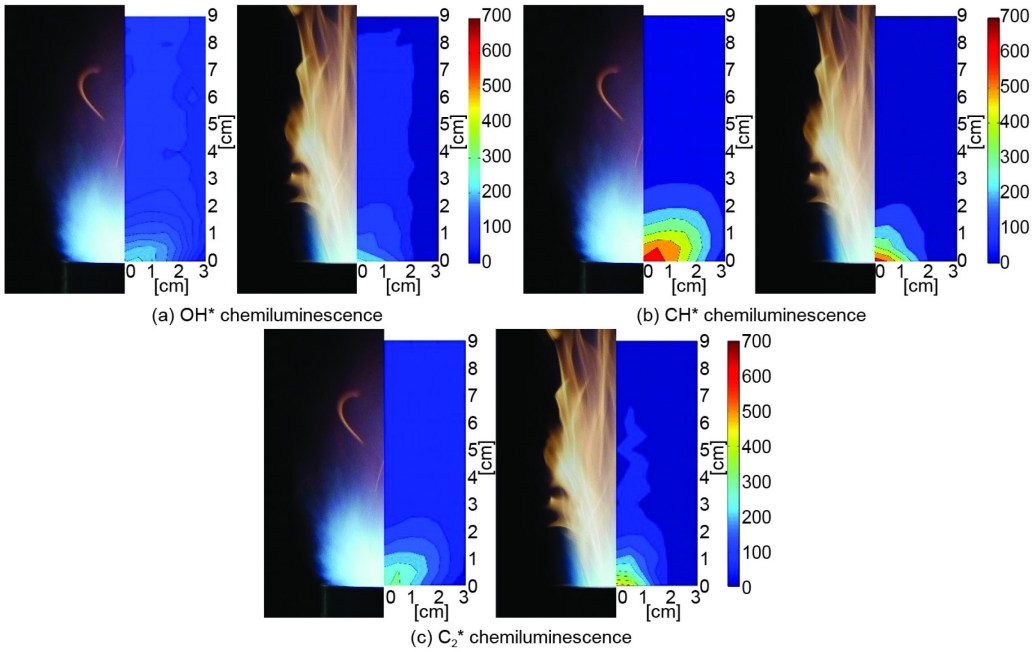

Figure 5. Raw OH*, CH*, C_2* chemiluminescence distribution with a comparison of steam blast (left) and air blast atomization (right) at a 0.7 bar atomization gauge pressure
(*for color image see journal web site*)

were relatively similar while C_2* and chemiluminescence intensity gradients were remarkably lower in the steam blast cases. The latter observation points out that the reaction rates were also lower, which can be explained by the differences in the above calculated adiabatic flame temperatures.

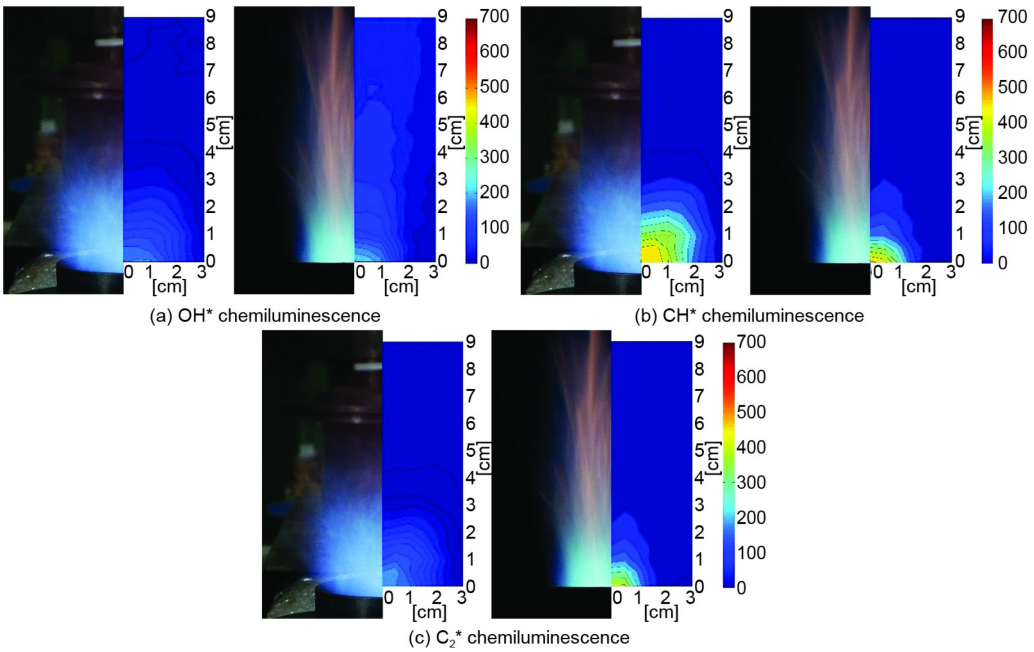

Figure 6. Raw OH*, CH*, C_2* chemiluminescence distribution with a comparison of steam blast (left) and air blast atomization (right) at a 1.0 bar atomization gauge pressure
(*for color image see journal web site*)

Investigation of intensity ratios

Chemiluminescence intensity ratio plots are not shown because the signal-to-noise ratio (SNR) drastically decreased in the horizontal direction which was expected due to the large gradients in the temperature and the excited radical concentrations. Vertically, the chemiluminescence intensities decreased in a remarkably lower extent. However, at 32.5 mm axial distance, the SRN become unity, and it increased further. Consequently, the investigated region is 2.5-27.5 mm downstream from the burner lip.

In the upcoming part, the best position for the spectrometer is investigated. There is no doubt that it should point at the axis of the burner. As for fluid fueled burners, the downstream distance of the control volume from the burner lip is not evident. The centrally injected droplets can be present in the near field of the axis even after the lip, hence, quenching the flame [23]. Figure 7 presents the corrected chemiluminescence intensities of OH*/CH*, OH*/C_2*, and CH*/C_2*. As for CH* and C_2* correction, intensity values at 450 nm and 528 nm were simply subtracted, similarly to the work of Docquier *et al.* [29]. The error bars indicate the uncertainty at 95% level of significance.

The OH*/CH* and OH*/C_2* chemiluminescence intensity ratios increase and become even more divergent with increasing axial distances. The previous one shows relatively similar chemiluminescence ratio of OH* and CH* just above the lip while the latter shows the

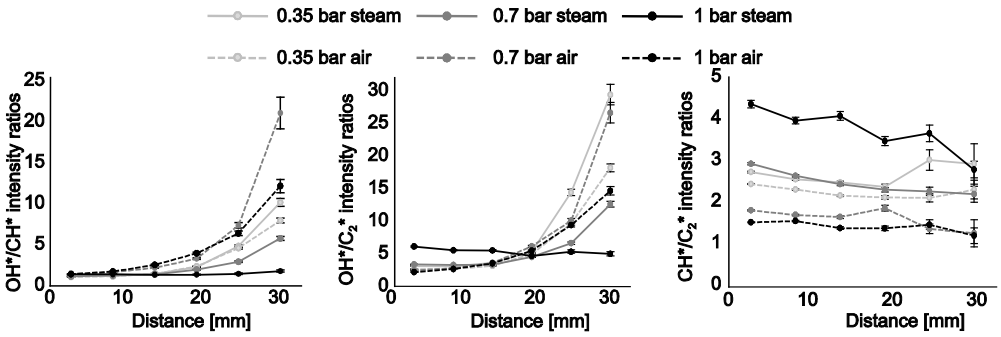

Figure 7. The OH*/CH*, OH*/C_2*, and CH*/C_2* chemiluminescence intensity ratios along the axis

closest ratios at 12.5 mm downstream from the lip. It can be stated that steam blast atomization at 1 bar gauge pressure is less sensitive to the sampling place. The SNR at 27.5 mm axial distance remains below 25% in each case, and it decreases to 6.5% at the flame root quadratically. The CH*/C_2* chemiluminescence intensity ratio is the most promising one whilst it showed only slightly descending characteristics generally with the growing axial distance for both air and steam blast atomization cases.

The mentioned flame quenching effect by the presence of fuel droplets proposed by Muruganandam *et al.* [23] have not exactly been observed in the current measurement series, possibly due to the mixing tube of the burner and a subsequent diverging nozzle after it. With increasing atomization pressure, both OH*/C_2* and CH*/C_2* chemiluminescence intensity ratios are lower in the air blast atomization cases and as an opposite, they are growing with increasing atomization pressure in the steam blast cases. As for air blast atomization, the reason could be the lower droplet sizes and hence lower evaporation timescales along with enhanced mixing, leading to more intense volumetric reactions at higher atomization pressures. The H_2O molecules can dissociate at high temperatures to H and O atoms which react in fast processes with the precursor radicals of C_2* thus reducing its concentration and so the intensity of its chemiluminescence [14]. As the atomization pressure increases, more steam is injected. Hence, the described effect lowers the C_2* intensity in a greater extent.

The analysis of the chemiluminescence intensity ratios of radicals reveals a strongly decreasing SNR with increasing axial distance, therefore installing a sensor too far from the burner lip may lead to poor results. Despite the analysis was carried out at 15 kW firing power, at higher performances the flame shape had the same height and width (not shown here), which is in agreement with the measurements of Kang *et al.* [38]. Therefore, the position of the spectrometer is as satisfactory at idle conditions as it is at full load if the combustion is fully turbulent, which is typical in most of the industrial-scale applications. Based on the measurement results, a chemiluminescence-based equivalence ratio sensor is recommended to be placed close to the lip of the burner to ensure a reliable operation and appropriate SNR.

Conclusions

An experimental analysis was conducted to measure and compare the steam blast atomization and air blast atomization of standard diesel oil in an atmospheric, LPP burner at 15 kW firing power by FES. Spatial contour plots of OH*, CH*, and C_2* chemiluminescence of the flames were presented. Along the axis, OH*/CH*, OH*/C_2*, and CH*/C_2* corrected

chemiluminescence intensity ratios were analyzed. Based on the measurements, the following conclusions can be derived.

- Steam blast atomization resulted in lower adiabatic flame temperature compared to air blast atomization. Therefore, the chemiluminescence intensity was generally reduced. The reduction of C_2* is not proportional to the reduction of OH* or CH* intensities. The more steam was added with steam blast atomization and the more significant decrease was observed.
- The diesel oil operated LPP burner resulted in no observable sign of quenching effect of droplets, as it was mentioned by Muruganandam *et al.* [23].
- The axial position of the spectrometer above the burner is critical: OH*/CH* and OH*/C_2* are quite sensitive to it. Furthermore, at the same air-to-fuel ratio the measurements resulted in diverging trends at different atomization gauge pressures with increasing axial distances. Interestingly, CH*/C_2* showed quite low sensitivity to the axial position, which indicates the similar chemiluminescent intensity of these excited radicals concerning both atomization mediums. However, the SNR is decreasing in parallel with the axial distance quadratically.

Acknowledgment

This research was supported by BUTE Department of Energy Engineering relating to the grant TAMOP-4.2.2.B-10/1-2010-0009. We are grateful for Attila Kun-Balog for supporting the experiments, Anett Horvath for the illustrations, Professor Assaad Masri, and Tamas Fulop for their useful insights.

References

[1] Lefebvre, A. H., Pollution Control in Continuous Combustion Engines, *Symp. Combust.*, *15* (1975), 1, pp. 1169-1180
[2] Sarofim, A. F., Flagan, R. C., NO_x Control for Stationary Combustion Sources, *Prog. Energy Combust. Sci.*, *2* (1976), 1, pp. 1-25
[3] Bowman, C., Control of Combustion-Generated Nitrogen Oxide Emissions: Technology Driven by Regulation, *Symp. Combust.*, *24* (1992), 1, pp. 859-878
[4] Furuhata, T., *et al.*, Effect of Steam Addition Pathways on No Reduction Characteristics in a Can-Type Spray Combustor, *Fuel*, *89* (2010), 10, pp. 3119-3126
[5] Pereira, C., *et al.*, Combustion of Biodiesel in a Large-Scale Laboratory Furnace, *Energy*, *74* (2014), Sept., pp. 950-955
[6] Bolszo, C. D., McDonell, V. G., Emissions Optimization of a Biodiesel Fired Gas Turbine, *Proc. Combust. Inst.*, *32* (2009), 2, pp. 2949-2956
[7] Lefebvre, A. Ballal, D. R., *Gas Turbine Combustion*, 3rd ed., CRC Press, Boca Raton, Fla., USA, 2010
[8] Law, C. K., Recent Advances in Droplet Vaporization and Combustion, *Prog. Energy Combust. Sci.*, *8* (1982), 3, pp. 171-201
[9] Lif, A., Holmberg, K., Water-in-Diesel Emulsions and Related Systems., *Adv. Colloid Interface Sci.*, *123-126* (2006), 2, pp. 231-239
[10] Breen, B., Combustion in Large Boilers: Design and Operating Effects on Efficiency and Emissions, *Symp. Combust.*, *16* (1977), 1, pp. 19-35
[11] Li, Z., *et al.*, Mixing and Atomization Characteristics in an Internal-Mixing Twin-Fluid Atomizer, *Fuel*, *97* (2012), Jul., pp. 306-314
[12] Correa, S. M., Power Generation and Aeropropulsion Gas Turbines: from Combustion Science to Combustion Technology, *Symp. Combust.*, *27* (1998), 2, pp. 1793-1807
[13] Dryer, F. L., Water Addition to Practical Combustion Systems – Concepts and Applications, *Symp. Combust.*, *16* (1977), 1, pp. 279-295
[14] Zhao, D., *et al.*, Behavior and Effect on NO_x Formation of OH Radical in Methane-Air Diffusion Flame with Steam Addition, *Combust. Flame*, *130* (2002), 4, pp. 352-360

[15] De Jager, B., *et al.*, The Effects of Water Addition on Pollutant Formation from LPP Gas Turbine Combustors, *Proc. Combust. Inst.*, *31* (2007), 2, pp. 3123-3130
[16] Meier, W., *et al.*, Detailed Characterization of the Dynamics of Thermoacoustic Pulsations in a Lean Premixed Swirl Flame, *Combust. Flame*, *150* (2007), 1-2, pp. 2-26
[17] Juddoo, M., Masri, A. R., High-Speed OH-PLIF Imaging of Extinction and Re-Ignition in Non-Premixed Flames with Various Levels of Oxygenation, *Combust. Flame*, *158* (2011), 5, pp. 902-914
[18] Lackner, M., *et al.*, In-Situ Laser Spectroscopy of CO, CH_4, and H_2O in a Particle Laden Laboratory-Scale Fluidized Bed Combustor, *Thermal Science*, *6* (2002), 2, pp. 13-27
[19] Ballester, J., Garcia-Armingol, T., Diagnostic Techniques for the Monitoring and Control of Practical Flames, *Prog. Energy Combust. Sci.*, *36* (2010), 4, pp. 375-411
[20] Guyot, D., *et al.*, CH*/OH* Chemiluminescence Response of an Atmospheric Premixed Flame under Varying Operating Conditions, *Proccedings,* ASME Turbo EXPO, Glasgow, UK, 2010, pp. 1-12
[21] Parameswaran, T., *et al.*, Gasification Temperature Measurement with Flame Emission Spectroscopy, *Fuel*, *134* (2014), Oct., pp. 579-587
[22] Romero, C., *et al.*, Spectrometer-Based Combustion Monitoring for Flame Stoichiometry and Temperature Control, *Appl. Therm. Eng.*, *25* (2005), 5, pp. 659-676
[23] Muruganandam, T. M., *et al.*, Optical Equivalence Ratio Sensors for Gas Turbine Combustors, *Proc. Combust. Inst.*, *30 I* (2005), 1, pp. 1601-1609
[24] Tripathi, M. M., *et al.*, Chemiluminescence-Based Multivariate Sensing of Local Equivalence Ratios in Premixed Atmospheric Methane-Air Flames, *Fuel*, *93* (2012), Mar., pp. 684-691
[25] Kojima, J., *et al.*, Basic Aspects of OH(A), CH(A), and C2(d) Chemiluminescence in the Reaction Zone of Laminar Methane-Air Premixed Flames, *Combust. Flame*, *140* (2005), 1, pp. 34-45
[26] Higgins, B., *et al.*, An Experimental Study on the Effect of Pressure and Strain Rate on CH Chemiluminescence of Premixed Fuel-Lean Methane/Air Flames, *Fuel*, *80* (2001), 11, pp. 1583-1591
[27] Higgins, B., *et al.*, Systematic Measurements of OH Chemiluminescence for Fuel-Lean, High-Pressure, Premixed, Laminar Flames, *Fuel*, *80* (2001), 1, pp. 67-74
[28] Parameswaran, T., *et al.*, Estimation of Combustion Air Requirement and Heating Value of Fuel Gas Mixtures from Flame Spectra, *Appl. Therm. Eng.*, *105* (2014), July, pp. 353-361
[29] Docquier, N., *et al.*, Closed-Loop Equivalence Ratio Control of Premixed Combustors Using Spectrally Resolved Chemiluminescence Measurements, *Proc. Combust. Inst.*, *29* (2002), 1, pp. 139-145
[30] Hwang, W., *et al.*, Spectroscopic and Chemical-Kinetic Analysis of the Phases of HCCI Autoignition and Combustion for Single- and Two-Stage Ignition Fuels, *Combust. Flame*, *154* (2008), 3, pp. 387-409
[31] Gordon, R. L., Mastorakos, E., Autoignition of Monodisperse Biodiesel and Diesel Sprays in Turbulent Flows, *Exp. Therm. Fluid Sci.*, *43* (2012), Nov., pp. 40-46
[32] Merola, S. S. S., *et al.*, Chemiluminescence Analysis of the Effect of Butanol-Diesel Fuel Blends on the Spray-Combustion Process in an Experimental Common Rail Diesel Engine, *Thermal Science*, 19 (2014), 6, pp. 1-20
[33] Chigier, N. A., The Atomization and Burning of Liquid Fuel Sprays, *Prog. Energy Combust. Sci.*, *2* (1976), 2, pp. 97-114
[34] Kun-Balog, A., Sztanko, K., Reduction of Pollutant Emissions from a Rapeseed Oil Fired Micro Gas Turbine Burner, *Fuel Process. Technol.*, *134* (2015), Jun., pp. 352-359
[35] Jozsa, V., Kun-Balog, A., The Effect of the Flame Shape on Pollutant Emission of Premixed Burner, *Proceedings,* European Combustion Meeting, Budapest, 2015, pp. 4-35
[36] Kovacs, V., *et al.*, Comparative Analysis of Renewable Gaseous Fuels by Flame Spectroscopy, *Proceedings,* 3rd European Combustion Meeting, Chania, Greece, 2007, pp. 1-4
[37] Jozsa, V., Kun-Balog, A., Spectroscopic Analysis of Crude Rapeseed Oil Flame, *Fuel Process. Technol.*, *139* (2015), Nov., pp. 61-66
[38] Kang, Y.-H., *et al.*, Experimental and Theoretical Study on the Flow, Mixing, and Combustion Characteristics of Dimethyl Ether, Methane, and LPG Jet Diffusion Flames, *Fuel Process. Technol.*, *129* (2015), Jan., pp. 98-112

Paper submitted: June 16, 2015
Paper revised: February 1, 2016
Paper accepted: March 7, 2016